ELSEVIER

Journal of Crystal Growth 170 (1997) 66–71

JOURNAL OF CRYSTAL GROWTH

Heat transfer and mass transport in a multiwafer MOVPE reactor: modelling and experimental studies

T. Bergunde [a,*], M. Dauelsberg [b], L. Kadinski [b], Yu.N. Makarov [b], M. Weyers [a], D. Schmitz [c], G. Strauch [c], H. Jürgensen [c]

[a] *Ferdinand-Braun-Institut für Höchstfrequenztechnik, Rudower Chaussee 5, D-12489 Berlin, Germany*
[b] *Lehrstuhl für Strömungsmechanik, Universität Erlangen-Nürnberg, Cauerstrasse 4, D-91058 Erlangen, Germany*
[c] *Aixtron GmbH, Kackerstrasse 15–17, D-52072 Aachen, Germany*

Abstract

An improved detailed model for the calculation of the temperature distribution in a multiwafer Planetary Reactor™ has been developed. The temperature field of the reactor has been calculated in dependence of the reactor parameters for (Al,Ga)As growth as well as on the kind and the thickness of the wall and susceptor deposits. The amount of parasitic wall deposits can be minimized by a proper tuning of the reactor temperature distribution. Calculated GaAs growth rate profiles on 3 inch wafers show a strong dependence on the temperature field in the reactor and the amount of parasitic deposits. These predicted relationships have been used to optimize the reactor temperature distribution in order to minimize parasitic wall depositions. By this procedure a growth rate uniformity of $< 1\%$ on 3 inch wafers can be reproducibly achieved.

1. Introduction

The multiwafer Aix-2000 Planetary Reactor™ for 7×2 inch is a widely used growth system for metalorganic vapour phase epitaxy (MOVPE) of various semiconductor device structures, which is especially suitable for large scale production due to the high degree of growth rate uniformity, process reproducibility and good utilization of precursor material [1]. Mathematical modelling has become useful for the investigation and understanding of the growth mechanism and for growth process optimization. In Refs. [2,3] the detailed dependence of growth rate distribution on diverse process parameters was studied experimentally and explained using modelling calculations. Meanwhile the mathematical model has been considerably improved as described in Ref. [4] allowing more detailed studies, which include for the first time details of reactor geometry, spectral dependence of radiative heat transfer and wall effects.

The subject of this work is the temperature distribution in the reactor and its interaction with growth for the 5×3 inch configuration. First the temperature distribution for typical reactor parameters and its interdependence with deposits formed on the wall and the susceptor during growth are described in detail. Then the effects of the temperature distribution on the AlGaAs growth rate are studied. The results of the modelling are utilized to improve and optimize the growth process.

* Corresponding author. Fax: +49 30 6392 2642; E-mail: bergunde@fbh.fta-berlin.de.

0022-0248/97/$17.00 Copyright © 1997 Elsevier Science B.V. All rights reserved
PII S0022-0248(96)00551-9

2. Mathematical modelling

The mathematical model is based on the two-dimensional solution of coupled partial differential equations describing conservation of total mass and momentum, conjugate heat transfer and the chemical species' convective and diffusive mass transport in the gas mixture [5]. Coupling of flow and the species' mass transport is crucial for predicting flow behaviour in the Planetary Reactor, because the local composition of the gas mixture is not uniform, especially near the entrance. The chemical model consists of multicomponent mass transport equations for the prevailing gas phase components including homogeneous decomposition reactions of the metalorganic precursor [6], thermodiffusion and kinetically limited reactions on the quartz walls as described in Ref. [3]. To predict the temperature distribution in the reactor, heat transfer calculations assuming non-gray radiative transfer through a non-participating medium with semitransparent diffusely reflecting walls [7,8] and partitioning of the thermal radiation wavelength spectrum into a series of finite bands are employed. The formation of deposits on the quartz ceiling and their influence on radiative properties of the wall due to interference effects for thin films and absorption and emission of radiation in thick films and the quartz wall [9] are taken into account.

The numerical scheme consists of a finite volume method using block-structured non-orthogonal collocated grids for two-dimensional coupled flow, heat transfer and mass transport. Convergence speed-up is achieved by employing a multigrid technique.

3. Experimental studies

(Al,Ga)As layers ($x = 0.2$–0.3) were grown from TMGa, TMAl and AsH_3 on 3 inch GaAs wafers in a multiwafer Planetary Reactor^{TM} Aix-2000 described in Ref. [3]. Growth temperature was between 650 and 750°C, reactor pressure was $p = 200$ hPa and the total flow rate F was varied between 11 and 17.2 slm. The ratio of the flow rates between the upper and the lower inlet channel $R = F(\text{upper})/F(\text{lower})$ was varied between 12 and 56. The temperature of the reactor ceiling was varied by changing the composition of a H_2/Ar cooling gas mixture and thus the thermal coupling to the water-cooled top of the reactor. The ceiling temperature was measured using a thermocouple at a fixed radial position through a hole in the reactor top of an upscaled Aix-2400 reactor. Particular attention was payed to a good thermal contact of the thermocouple tip to the ceiling surface. Calculations and comparable experiments for the Aix-2000 and the larger Aix-2400 reactor show that the obtained results are valid for both geometries.

Growth rate profiles on static and rotating wafers in dependence of the growth parameters were obtained from reflectance maps at room temperature in a SPM-200 mapper. Demanding a difference of the refractive index between the substrate and the layer only ternary layers could be measured. As the uniformity of layer composition was generally at the resolution limit of luminescence and X-ray measurements ($\pm 0.1\%$) it could be concluded that the Al and Ga precursors show the same reactor transport behaviour under the observed growth conditions. Calculated composition values fit well the measured ones. Therefore, the modelling results will be shown for GaAs only; growth rate values and uniformities of AlGaAs are easily obtained by scaling.

4. Results and discussion

For typical growth conditions the temperature distribution in the reactor was calculated as shown in Fig. 1 (inset). From these calculations the temperature profile on the inner and outer of the ceiling can

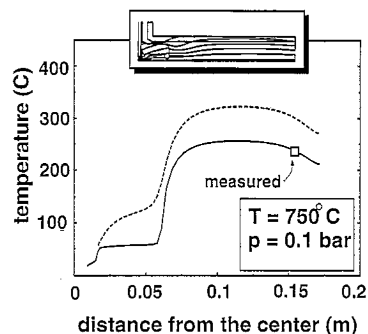

Fig. 1. Calculated ceiling temperature distributions in the Planetary Reactor AIX-2400 for the case of a clean ceiling, compared with the temperature (□) measured at a fixed position with a thermocouple. (---) Lower side of the quartz wall. (———) Upper side. Inset: Isolines ($\Delta T = 100$°C) of the calculated temperature distribution.

be extracted (Fig. 1). The calculated value for the outside is well in agreement with the measured one.

4.1. Ceiling temperature effects

The coating of both ceiling and susceptor with deposits has pronounced effects on the temperature distribution in the reactor, although the amount of deposits on the ceiling is orders of magnitude below the susceptor coating. Dielectric semitransparent polycrystalline GaAs layers formed on a relatively hot ceiling cause a decrease of the calculated ceiling temperature of up to about 50°C at film thicknesses of up to a few hundred nanometres due to interference phenomena (Fig. 2a). Beyond a film thickness of 500 nm interference has a lower effect. For thicknesses over several μm absorption of thermal radiation in the GaAs film becomes dominant over absorption in the quartz wall resulting in ceiling temperatures above that of the clean ceiling. At optimized growth conditions, however, this amount of ceiling deposition is not reached. If the ceiling is

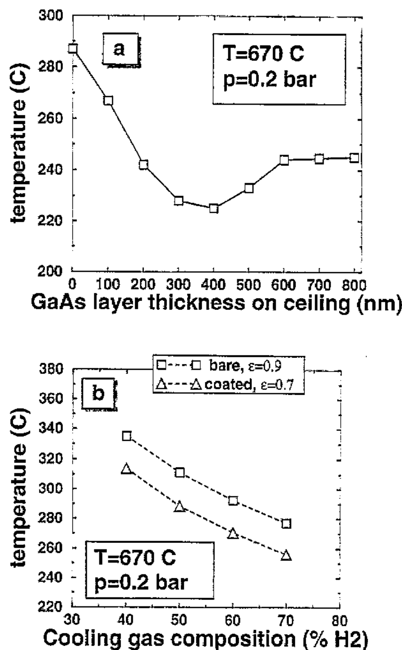

Fig. 2. Dependence of the calculated maximum ceiling temperature in the Planetary Reactor AIX-2000 on (a) the thickness of GaAs coating on the ceiling, and (b) on cooling gas composition for two susceptor emittances. (□) $\epsilon_s = 0.9$, (△) $\epsilon_s = 0.7$, corresponding to the case of a pure graphite surface and graphite covered by a thick layer of GaAs, respectively.

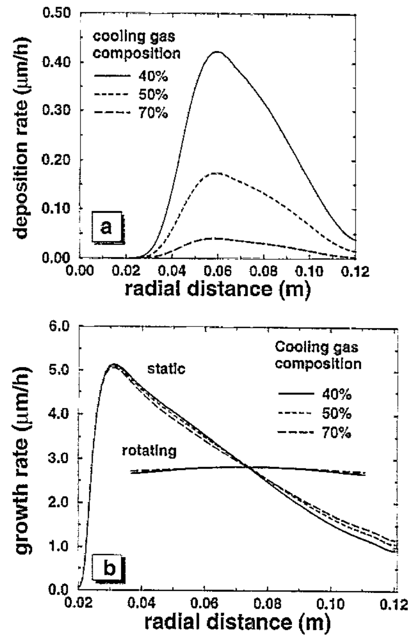

Fig. 3. (a) Calculated GaAs deposition rates on the ceiling plate at various compositions of the ceiling cooling gas mixture (H_2/Ar) in the Planetary Reactor AIX-2000. ($T = 670°C$, $p = 0.2$ bar). (b) Calculated GaAs growth rate profile on a static and rotating susceptor for these conditions.

relatively cold metallic arsenic can condense. Owing to the high reflectivity of this metallic surface the ceiling temperature drops drastically to a value which is 100°C below that obtained for a thin GaAs coating. This cooling then enhances As deposition further. In agreement with the calculations an optimized adjustment of the cooling rate at the ceiling was found to minimize any deposits almost to zero. Adjacent to the deposition-free temperature range, black, opaque As deposits indicate a too low temperature, a dense brownish GaAs film is deposited at temperatures above the optimum. Deposition rates of polycrystalline GaAs on the ceiling were calculated for various ceiling cooling rates including also non-optimal conditions (Fig. 3a). Due to the Arrhenius-like dependence of the rate of kinetically limited deposition on temperature, an approximately exponential reduction of the deposited layer thickness with a linear increase of the cooling rate occurs. According to Fig. 2a thin (Al,Ga)As deposits on the ceiling can be expected to act self-stabilizing, because they lower the ceiling temperature, and thus the parasitic deposition rate, whereas thick deposits

on the ceiling lead to an unstable, increasing ceiling temperature and deposition rate due to rising radiation absorption. A further factor influencing the temperature profile in the reactor is the coating of the graphite susceptor, which leads to a reduced surface emittance. During GaAs growth the emittance decreases from 0.9 for pure graphite to about 0.7 for several tens of μm of grown layer thickness. This causes a drop of ceiling temperature of about 25°C for any cooling gas composition (Fig. 2b). To compensate for this drift the temperature of the ceiling is adjusted via the cooling gas composition. This allows for stable operation starting from a clean susceptor up to an accumulated growth of more than a hundred μm. The modelling results have been used to implement an active ceiling temperature controller (±0.1°C) that compensates the drift in heat irradiation due to changing surface emittance of the susceptor during ongoing multilayer processes and keeps the ceiling in the optimized temperature range where it stays free from deposits. It has now been achieved for the first time that the entire boundary conditions in an MOVPE reactor are automatically controlled.

4.2. Growth rate effects

Changes in the reactor temperature field directly affect the growth rate distribution on the susceptor. Fig. 3b shows how calculated growth rate profiles depend on the cooling gas composition above the ceiling due to competing material losses on the ceiling, as shown in Fig. 3a. At a hydrogen content below 40% in the cooling gas a remarkable decrease of the downstream side of the growth rate profile is observed. The enhancement of diffusive transport by a hotter reactor environment at low cooling rates slightly increases the growth rate on the upstream side. Due to both effects the resulting growth rate profile on a rotating wafer becomes more convex. This effect has been verified experimentally at 650 and 750°C.

In addition to the ceiling temperature adjustment, as described above, the temperature profile was locally varied in the central area of the reactor near the gas inlet by adjusting the heat flux density from the IR-heater unit. As seen from Fig. 4 a lowering of the temperature in the centre by $\Delta T = -100$°C leads to a remarkable increase of the growth rates upstream of the wafer due to decreased losses in the central

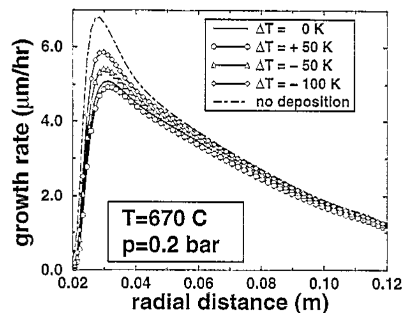

Fig. 4. Calculated GaAs growth rate profiles for a temperature variation ΔT only in the centre of the reactor. The limiting case of growth without deposition loss is also given.

area. For comparison a depletion profile without any parasitic losses is shown. In our growth experiments we found that this effect is the primary factor affecting the rate profile. It has been found that a variation of the temperature-dependent diffusivities of the group-III precursors that determine the growth rate changes the growth rate profile only in its medium part slightly in the absence of competing ceiling deposits (see Fig. 3). Only in the case of a drastic temperature decrease associated with an arsenic coverage of the ceiling is the growth rate influenced remarkably. The general shape of the growth rate profile is preserved. Under optimized practical growth conditions, i.e. in the absence of ceiling deposits and with a controlled ceiling temperature, the effect of the temperature profile on diffusive transport plays only a subordinate role.

Thus, the shape of the different parts of the growth rate profile on a static susceptor can be directly attributed to three different influences: to the temperature in the inlet region and the resulting losses (upstream part), to the temperature in the reactor volume (medium part) and to possible ceiling deposits (downstream part). A growth rate profile free from material losses has been achieved by the control and use of these interactions. This is demonstrated in Fig. 5. In the case of a non-optimized reactor temperature distribution, accumulating wall depositions shift the temperature field within the first runs creating an increasing loss in the upstream growth rate profile. The rotating profile switches from concave to convex and the homogeneity deteriorates in the further runs. In the case of an optimized temperature distribution the formation of reactor wall

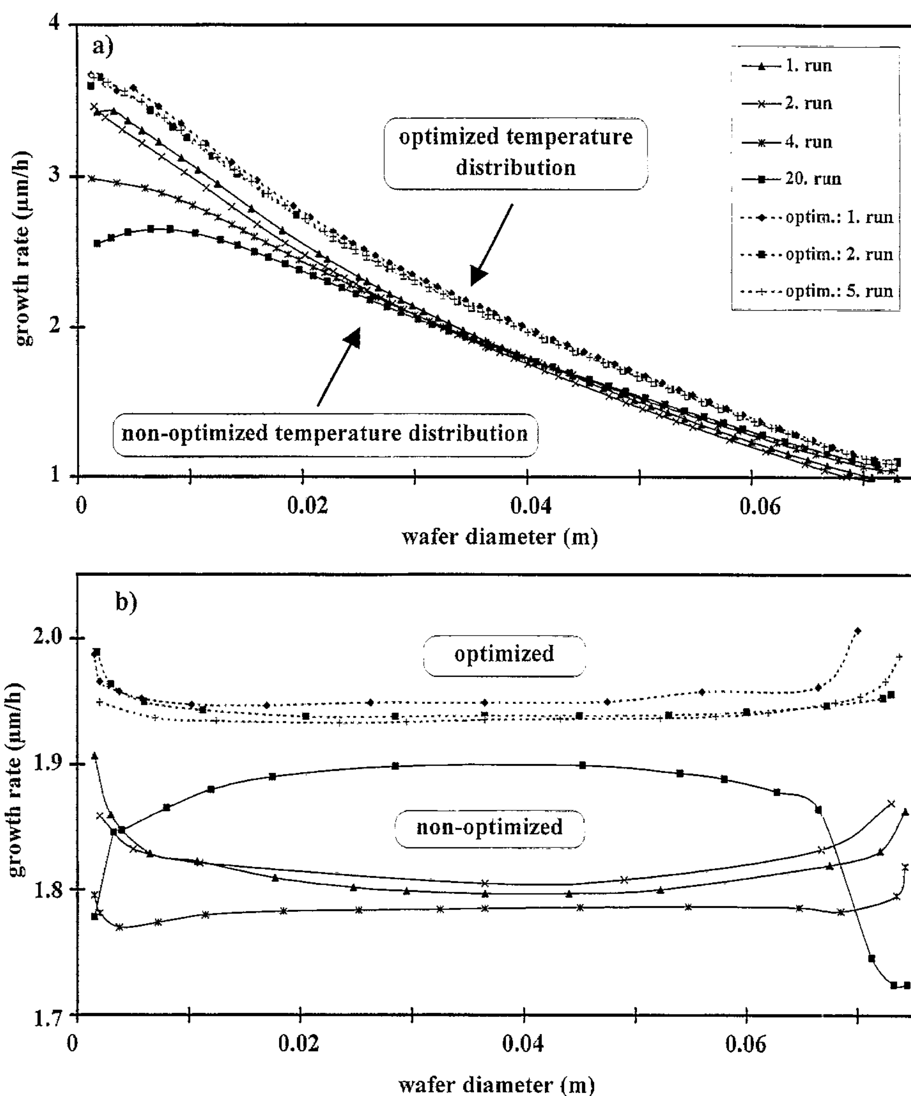

Fig. 5. Comparison of the (a) static and (b) rotating growth rate profiles for non-optimized and optimized reactor temperature distributions.

deposits is minimized and layers with a constant depletion profile on static wafers are grown. A growth rate uniformity of $< 1\%$ on rotating 3 inch wafers is reproducibly achieved.

5. Conclusions

An improved detailed model for the calculation of the temperature distribution in a multiwafer Planetary Reactor^{TM} has been developed. The temperature field of the reactor has been calculated in dependence of the reactor parameters as well as on the kind and the thickness of the wall and susceptor deposits. The obtained results agree well with the experimental findings. The amount of parasitic wall deposits can be minimized by a proper tuning of the reactor temperature, which is in turn remarkably influenced by the deposits. Calculated GaAs growth rate profiles on 3 inch wafers show a strong dependence on the temperature field in the reactor and the amount of parasitic deposits. These predicted rela-

tionships have been used to optimize the reactor temperature distribution in order to minimize parasitic wall depositions. Thus a growth rate uniformity of $< 1\%$ on 3 inch wafers has been obtained reproducibly.

Acknowledgements

The contributions of V.S. Yuferev, A.F. Ioffe Physical Technical Institute, St. Petersburg, to modelling of radiative heat transfer are highly appreciated.

References

[1] P.M. Frijlink, J.L. Nicolas, H.P.M.M. Ambrosius, R.W.M. Linders, C. Waucquez and J.M. Marchal, J. Crystal Growth 115 (1991) 203.
[2] T. Bergunde, F. Durst, L. Kadinski, Yu.N. Makarov, M. Schäfer and M. Weyers, J. Crystal Growth 145 (1994) 630.
[3] T. Bergunde, D. Gutsche, L. Kadinski, Yu.N. Makarov and M. Weyers, J. Crystal Growth 146 (1995) 564.
[4] T. Bergunde, M. Dauelsberg, Yu. Egorov, L. Kadinski, Yu.N. Makarov, M. Schäfer, G. Strauch and M. Weyers, in: Simulation of Semiconductor Devices and Processes, Vol. 6, Eds. H. Ryssel and P. Pichler (Springer, New York, 1995) pp. 328–331.
[5] C.R. Kleijn, Chemical vapor deposition processes, in: Computational Modelling in Semiconductor Processing, Ed. M. Meyyappan (Artech House, 1995) ch. 4, pp. 97–230.
[6] C.A. Larsen, N.I. Buchan, S.H. Li and G.B. Stringfellow, J. Crystal Growth 102 (1989) 103.
[7] L. Kadinski and M. Perić, Int. J. Num. Meth. Heat Fluid Flow 6 (1996), to be published.
[8] F. Durst, L. Kadinski and M. Schäfer, J. Crystal Growth 146 (1995) 202.
[9] L. Kadinski, Y.N. Makarov, M. Schäfer, V. Yuferev and M. Vasil'ev, J. Crystal Growth 146 (1995) 209.